




Transpulmonary amino acid metabolism in the sugen hypoxia model of pulmonary hypertension

Nicolas Philip¹ | Hongyang Pi² | Mahin Gadkari³  | Xin Yun¹ | John Huetsch¹ | Cissy Zhang⁴ | Robert Harlan³ | Aurelie Roux³ | David Graham³ | Larissa Shimoda¹ | Anne Le⁴ | Scott Visovatti⁵ | Peter J. Leary² | Sina A. Gharib² | Catherine Simpson¹  | Lakshmi Santhanam³ | Jochen Steppan³ | Karthik Suresh¹ 

¹Division of Pulmonary/Critical Care Medicine, Baltimore, Maryland, USA

²Division of Pulmonary, Critical Care and Sleep Medicine, University of Washington, Seattle, Washington, USA

³Department of Anesthesiology and Critical Care Medicine, Johns Hopkins University School of Medicine, Baltimore, Maryland, USA

⁴Department of Pathology, Johns Hopkins University School of Medicine, Baltimore, Maryland, USA

⁵Division of Cardiology, Ohio State University School of Medicine, Columbus, Ohio, USA

Correspondence

Karthik Suresh, Division of Pulmonary/Critical Care Medicine, 5501 Hopkins Bayview Cir, Baltimore, MD 21228, USA.
 Email: ksuresh2@jhmi.edu

Funding information

NIH, Grant/Award Numbers: K08HL132055, K08HL133475, K08HL145132, K23HL153781, R01HL126514, R01HL151530

Abstract

In pulmonary artery hypertension (PAH), emerging evidence suggests that metabolic abnormalities may be contributing to cellular dysfunction in PAH. Metabolic abnormalities such as glycolytic shift have been observed intracellularly in several cell types in PAH, including microvascular endothelial cells (MVECs). Concurrently, metabolomics of human PAH samples has also revealed a variety of metabolic abnormalities; however the relationship between the intracellular metabolic abnormalities and the serum metabolome in PAH remains under investigation. In this study, we utilize the sugen/hypoxia (SuHx) rodent model of PAH to examine the RV, LV and MVEC intracellular metabolome (using targeted metabolomics) in normoxic and SuHx rats. We additionally validate key findings from our metabolomics experiments with data obtained from cell culture of normoxic and SuHx MVECs, as well as metabolomics of human serum samples from two different PAH patient cohorts. Taken together, our data, spanning rat serum, human serum and primary isolated rat MVECs reveal that: (1) key classes of amino acids (specifically, branched chain amino acids—BCAA) are lower in the pre-capillary (i.e., RV) serum of SuHx rats (and humans); (2) intracellular amino acid levels (in particular BCAAs) are increased in SuHx-MVECs; (3) there may be secretion rather than utilization of amino acids across the pulmonary microvasculature in PAH and (4) an oxidized glutathione gradient is present across the pulmonary vasculature, suggesting a novel fate for increased glutamine uptake (i.e., as a source of glutathione). in MVECs in PAH.

Jochen Steppan and Karthik Suresh are co-senior authors.

This is an open access article under the terms of the Creative Commons Attribution-NonCommercial License, which permits use, distribution and reproduction in any medium, provided the original work is properly cited and is not used for commercial purposes.

© 2023 The Authors. *Pulmonary Circulation* published by John Wiley & Sons Ltd on behalf of Pulmonary Vascular Research Institute.

In summary, these data reveal new insight into the shifts in amino acid metabolism occurring across the pulmonary circulation in PAH.

KEYWORDS

amino acid metabolism, endothelial cells, metabolomics, PAH

INTRODUCTION

Pulmonary artery hypertension (PAH) is a morbid disease characterized by progressive elevation of pulmonary artery and right ventricular pressures, leading to heart failure and death. Increased lung microvascular endothelial cell (MVEC) proliferation is a key feature of the pathobiology of PAH. Studies of the mechanisms underlying MVEC proliferation in PAH have suggested that PAH MVECs adopt a pseudo-oncogenic phenotype, characterized by increased proliferation, and metabolic abnormalities.^{1,2} The metabolic abnormalities in PAH MVECs have garnered increased attention due to the possibility of interrupting these pathways through either dietary interventions or inhibition of import of various metabolic fuels (such as glucose, amino acids, or fatty acids) into MVECs. One specific metabolic abnormality that has been well documented in human endothelial cell cultures and animal models of PAH is glycolytic shift.^{3,4} Glycolytic shift occurs when carbons from glucose are shunted toward anaerobic respiration and generation of macromolecules critical for cellular proliferation and redox balance (e.g., nucleotides, NADPH). This leads to a relative decrease in the amount of glucose that is used to generate Acetyl-CoA and fuel the tricarboxylic acid (TCA) cycle. The metabolic response to glycolytic shift typically involves increased uptake of alternative fuels to replenish critical metabolites (anaplerosis). In MVECs cultured from a rat model model of PAH (the SU5416/Hypoxia model of PAH), we recently observed such glycolytic shift and anaplerosis;⁵ however, the compensation mechanisms that occur in response to the observed glycolytic shift in MVECs in PAH remains unclear, and whether such compensation is supported by one of more specific fuel sources is unknown.

In proliferative cells, anaplerotic carbons can be provisioned by a variety of non-glucose fuels, including fatty acids and amino acids. In addition to anaplerosis, amino acids are also required for protein synthesis, which is often accelerated under conditions of increased proliferation. In addition, the amino acid glutamine is needed to synthesize glutathione, a critical molecule that provides antioxidant capacity. Thus, the compensatory metabolic response to glycolytic shift is

complex, with competing demands on nutrients such as amino acids.

In addition to various intracellular demands for non-glucose fuels, there is also a supply side component to nutrient catabolism. Import of nutrients like amino acids and fatty acids from the serum into MVECs is an obligatory step; however, this aspect of metabolism is insufficiently captured in vitro, since these studies are often conducted in cultured cells. This is particularly significant with regard to essential amino acids (EAA); that is, amino acids that cannot be synthesized de novo by humans, and thus have to be absorbed via the gut and subsequently imported into ECs. By measuring serum metabolites in the PA and the aorta in PAH patients, Chouvarine et al. recently observed not only that metabolite gradients exist across the pulmonary circulation, but that certain metabolite levels (such as acetyllysine) actually increase across this circuit.⁶ This finding suggests the intriguing possibility that the lung may serve as a secretory organ with regard to metabolites. However, how such metabolite gradients relate to intracellular metabolite changes in PAH ECs remains unclear.

To address this question, we paired serum metabolomics with intracellular metabolomics performed on primary MVECs isolated from PAH and control animals. We hypothesized that in PAH, consumption of key metabolites by the pulmonary circulation would be reflected in the serum as follows: we predicted that metabolite levels of amino acids would be lower in the LV compared to the RV, and that this decrease would be accompanied by a concomitant increase in intracellular SuHx-MVEC amino acid levels, reflecting increased consumption.

METHODS

SuHx animal model

All procedures were approved by the Johns Hopkins University School of Medicine Animal Care and Use Committee. Procedures were conducted in accordance with the NIH *Guide for Care and Use of Laboratory Animals* as well as ARRIVE guidelines. SU5416 (Tocris, Bio-Techne) was prepared in a diluent composed of

dimethyl sulfoxide and carboxymethylcellulose as previously described.² Male Wistar rats (250–300 g) were injected subcutaneously with 20 mg/kg of SU5416 before exposure to sustained hypoxia (FiO₂ 0.1) for 3 weeks followed by return to normoxia (room air, FiO₂ 21%) for 2 weeks. Normoxic controls were treated with vehicle and were maintained in racks adjacent to the hypoxia chamber, at room air, for 5 weeks.

Hemodynamics

Closed-chested RV measurements were performed after 5 weeks in SUHx and control animals as described previously.⁷ Following anesthesia, a small mid-line abdominal incision was created to visualize the diaphragm. A 23-gauge needle flushed with heparinized saline was used to access the RV transdiaphragmatically and advanced into the RV. Tracings were obtained and analyzed as previously described.⁸ Hemodynamics, metabolomic extraction, and metabolomic analyses were done in a blinded fashion.

Metabolomics

Specimen acquisition

1. MVEC isolation: After hemodynamic measurements, peripheral strips of rat lung were excised and digested using Type 1A Collagenase as previously described.^{9,10} Briefly, the lung tissue was minced and digested before being incubated with CD31-coated beads to obtain a selection of CD31⁺ cells. As prior studies have shown that lung MVECs can be further identified based on positivity for *Griffonia simplicifolia* I, isolectin 4B (GS),¹¹ CD31⁺ cells were then subjected to a second magnetic-bead isolation using a GS antibody to isolate MVECs. We have previously phenotyped MVECs isolated using this process to confirm purity and MVEC origin.⁷ CD31⁺GS⁺ cells were subsequently grown to confluence in T75 flasks. All cells were used at passage 4. Control (i.e., normoxic) cells were phenotyped at every passage to ensure lack of transdifferentiation, as previously described.⁷ For select experiments, the CD31⁺GS⁻ fraction was saved, cultured in media and used, also at passage 4.
2. Cell culture/lysate collection for metabolomics: Cells and media were routinely tested for Mycoplasma contamination (Mycoalert, Lonza). The media used during isolation and subsequent growth of ECs consisted of the following components: Lonza

endothelial basal media (EBM) basal medium (CC-3156), fetal bovine serum (FBS) (Hyclone; 10% for growth media; 5% for basal media) and EGM2-MV Supplement (CC-4147) without hydrocortisone. Growth media (i.e., 10% FBS) was used during the initial isolation phase until cells were frozen (P3). Experiments using cultured cells were performed in basal media (5% FBS). All cells were grown on cultureware treated with 0.1% gelatin. For metabolomics cell lysate harvest, confluent T75 flasks of normoxic (N)-MVECs and SuHx-MVECs were harvested, washed with ice-cold PBS x 3, and then subjected to metabolite extraction using 80% (vol/vol) mass spectrometry-grade methanol in mass spectrometry-grade water followed by immediate storage at –80 degrees.

3. Individual metabolite measurements in cell culture media: P4 N- and SuHx MVECs were grown to confluence in T75 flasks. 24 h before harvest, the media (Lonza EBM based media, as described above) was changed. 24 h later, the media was collected, and a BCA assay was performed for protein quantification. Branched chain amino acid (BCAA), total glutathione and reduced glutathione levels in the media supernatant were measured using colorimetric assays (Abcam, BCAA: acb83374; GSH: ab239709). Oxidized glutathione was determined by subtracting the reduced glutathione value from total. Values were normalized for protein level obtained from the BCA assay. Data were analyzed using GraphPad Prism.
4. Serum: After closed-chested (i.e., transdiaphragmatic) right ventricular systolic pressure (RVSP) measurement, the chest cavity was opened via sternotomy. Open chested RVSP measurements were made and blood was subsequently drawn from the RV. The LV pressures were also measured and blood was drawn from this chamber. The samples were spun at 3000 rpm for 12 min and the serum was collected from the fractionated sample.

Mass spectrometry approach

1. Untargeted intracellular metabolomics—rat: Sample preparation of cell lysates for untargeted intracellular metabolomics was initiated by first removing the methanol from samples using a speed vacuum, and the water removed via lyophilization. Fifty percent (vol/vol) acetonitrile in mass spectrometry-grade water was used to re-suspend the lyophilized metabolites to generate the final sample for data acquisition. Data acquisition was performed using a Thermo Fisher Scientific Q Exactive Plus Orbitrap

Mass Spectrometer and a Vanquish Ultra Performance Liquid Chromatography (UPLC) system. The samples were maintained at 4°C inside the Vanquish UPLC auto-sampler, which drew 2 µL of sample for each injection. Reverse phase chromatography using a Discovery® HS F5 HPLC Column was used. The mobile aqueous phase was 0.1% formic acid in mass spectrometry-grade water and the mobile organic phase was 0.1% formic acid in 98% acetonitrile. The column and the column guard were kept at 35°C. Acquired data were analyzed using Thermo Fisher Scientific Compound Discoverer® and Thermo Fisher Scientific TraceFinder® software. The normalized intensities were obtained by normalizing the raw intensities, which were obtained by integrating the chromatographic peaks, to the protein concentration of each sample. Other LC/MS parameters were set as previously reported.⁵

2. Targeted serum and intracellular metabolomics—rat: For these studies, fragmentation patterns were determined using a known standard for each compound. Serum sample preparation was performed by mixing 25 µL of serum with 75 µL of water (Fisher Chemical Optima™ LC/MS, W6) and 300 µL of ice-cold acetonitrile (Fisher Chemical) and filtered using Supelco 96-Well Protein Precipitation Filter Plate (Sigma Aldrich). 10 µL of each filtered sample was pooled together into a quality control (QC) POOL to be run alongside the samples at regular intervals. 25 µL of filtrate was further diluted with 175 µL of water, vortexed, and centrifuged for 15 min at 10,000g. 5 µL of this dilution was injected on the mass spectrometer for analysis. Cell extracts aliquot of 1 mL methanol/water 80:20 (vol/vol) were dried down in a speed vacuum, then reconstituted in 100 µL of mass spectrometry-grade water for data acquisition. Before dry down 150 µL aliquot of each sample was pooled together into a QC POOL to be run alongside the samples at regular intervals. Two and 5 µL was injected on the mass spectrometer for analysis. Liquid chromatography-mass spectrometry (LC-MS) was accomplished by injecting samples, blanks, and QC Pools with an injection volume of 2–5 µL onto the LC-MS system. High pressure liquid chromatography (HPLC) was accomplished using a Shimadzu HPLC comprised of a SIL-30ACMP 6-MTP Autosampler, and Nexera LC-30AD HPLC Pumps (Shimadzu). Chromatographic separation was performed using a pentafluorophenylpropyl column with dimensions 150 × 4.6 mm ID, 3 µM particle size (Sigma, 567503-U). Mobile phase A: water and 0.1% formic acid and mobile phase B: acetonitrile with 0.1% formic acid. Gradient: 2% mobile phase B from 0 to 2 min, then

ramped to 25% mobile phase B from 2 to 5 min, then ramped to 35% mobile phase B from 5 to 11 min, and then ramped to 65% mobile phase B from 11 to 17 min, and equilibrated at 2% B for 2 min. Mass spectrometry was performed by a triple quadrupole mass spectrometer (Shimadzu, LCMS-8060) equipped with an electrospray ionization source used in both positive and negative mode. Resolution was set to 1 Dalton. Source conditions were set with nebulizing gas flow at 3 L/min, heating gas flow set to 10 L/min, interface temperature set to 300°C, DL temperature set to 250°C, heat block temperature set to 400°C, and drying gas flow set to 10 L/min. Each batch of samples was run with a System Suitability QC, which was created from commercially available plasma, and extracted in our laboratory using the sample preparation method described above. The purpose of this system suitability QC was to act as a purely analytical control that assures proper operation of the entire of LC-MS instrumentation from the HPLC components to the mass spectrometer. The result of this QC sample was determined by the response of known metabolites in the system suitability QC, which were evaluated for retention time, raw signal, peak shape, and chromatographic resolution. Sample batches that passed QC analysis, were then used in metabolite analyses. Chromatographic integration was performed by software Labsolutions Insight (Version 3.5).

Data analysis

Metabolomics analysis was conducted using the *MetaboAnalystR* package in R. Metabolomics data were scaled using Pareto Scaling (mean-centered and divided by the square root of the standard deviation of each variable) for multivariate analysis. Missing values were replaced by one fifth of minimum positive value in the original data, per metabolite.

Rat serum and intracellular lysate data

Overall differences between groups were evaluated by principal component analysis. Addition metabolite-specific contributions were determined using partial least squares discriminant analysis (PLS-DA). Variable Importance in Projection (VIP) scores were calculated using PLS-DA components. For all of these dimension reduction techniques, we represent the data as a function of principal components (PCs), which represent linear combinations of the measured metabolites. This allows

for determination of intergroup differences. Then, we calculate VIP scores to determine which specific metabolites are contributing most to the differences seen.

Human cohort #1 (serum metabolomics of SSC patients with and without PAH)

Human serum metabolomics and associated clinical annotation data were obtained via Metabolomics Workbench, Project ID: PR000551. The full metabolomics workflow used to obtain data for this study is provided online at the project webpage at metabolomicsworkbench.org. In this study, untargeted metabolomics were performed on a cohort of patients comprised of controls and Scleroderma (Scl) patients with and without PAH. The diagnosis of PAH in the Scl patients was made by either echocardiography or right heart catheterization (RHC). For the purposes of these analyses, we only included Scl patients with PAH and Scl patients without any evidence of PAH (based on echo/RHC). Scl patients often have gut involvement, and thus we reasoned that it was most appropriate to compare Scl+PAH- patients with Scl+PAH+ patients since amino acids levels between control (i.e., Scl-) and Scl+ patients may be confounded by differences in nutrient absorption between these two groups. Patients with “borderline pressures” were excluded from the analyses. The majority of the patients in this cohort were female, consistent with the epidemiology of Scl-PAH. There were too few male patients in this data set to stratify by sex; thus, we only used the female patient data. Available data included metabolite measurements in both the positive and negative ion modes; both were analyzed using the same workflow.

Human cohort #2 (serum metabolomics in patients with varying PAH severity)

The Servetus study is a single institution cohort of PAH participants enrolled between 2014 and 2016. For the current analysis, 74 participants had available right heart catheterization with reported RVSP, age, sex and physician confirmed etiology of PAH. Metabolites were characterized using ultrahigh-performance liquid chromatography-tandem mass spectroscopy analysis on plasma samples (Metabolon, Inc). Metabolomics data was preprocessed and normalized in the R statistical environment (R Core Team 2020). Metabolites were measured as area under the peak curve, normalized to run-day medians, and log₂-transformed. For the current analyses, 85 metabolites were included based on Metabolon annotation to be linked to Valine, leucine, isoleucine, phenylalanine and glutamine metabolism.

Linear regression was used to estimate relationships between metabolites and RVSP. Unadjusted analyses were considered. Adjusted models accounted for differences in age, sex at birth, BMI, and PAH etiology. Metabolites associated with RVSP with a *p*-value < 0.05 were considered as potentially significant.

For all the clustering analyses, a VIP score cut-off was 1.0 was used to define metabolites of interest.

Hemodynamic and specific metabolite data are presented as mean ± standard error and compared using an unpaired *t*-test, *p* < 0.05 was considered significant. The rat metabolomics raw data is provided in the data supplement (Supporting Information: Data 1).

RESULTS

SuHx exposure resulted in increased RVSP, right ventricular hypertrophy, increased RV/body weight, and an increased RV/LV + S weight (S: septum), consistent with severe pulmonary hypertension (Figure 1).

Next, we performed targeted metabolomics on serum collected from the RV of normoxic and SuHx rats at the time of hemodynamic measurements. After quality control (see methods), a total of 93 metabolites were included in the analysis. Principal components analysis of Normoxic and SuHx RV serum samples revealed clear differences between the two groups (Figure 2a). To determine specific metabolites that might be contributing to this difference between groups, we performed PLS-DA and calculated VIP scores (see Methods for details). As shown in the VIP plot (Figure 2b) as well as box plots of individual metabolites (Figure 2c), the differences between Normoxic- and SuHx- RV sera were driven primarily by lower metabolite levels of several amino acids in SuHx. Aside from glutamine, many of the other amino acids (such as valine, tryptophan, phenylalanine and histidine) were essential amino acids. The top metabolite that distinguished normoxic and SuHx RV samples was valine, an EAA that is also a branched chain amino acid (BCAA). Several other essential BCAA and their metabolites (norleucine, leucine, isoleucine) were also lower in SuHx RV serum.

This was an unanticipated finding, as we did not expect baseline differences in amino acids in the pre-capillary circulation. Given these findings, we reasoned that the lower levels of these metabolites could reflect either: (a) circulating low serum levels due to consumption of these metabolites within the pulmonary circulation, or (b) decreased availability of these metabolites to the pulmonary circulation (due to extrapulmonary effects of SuHx on amino acid mobilization from muscle and/or absorption of these metabolites from the gut). Thus, we

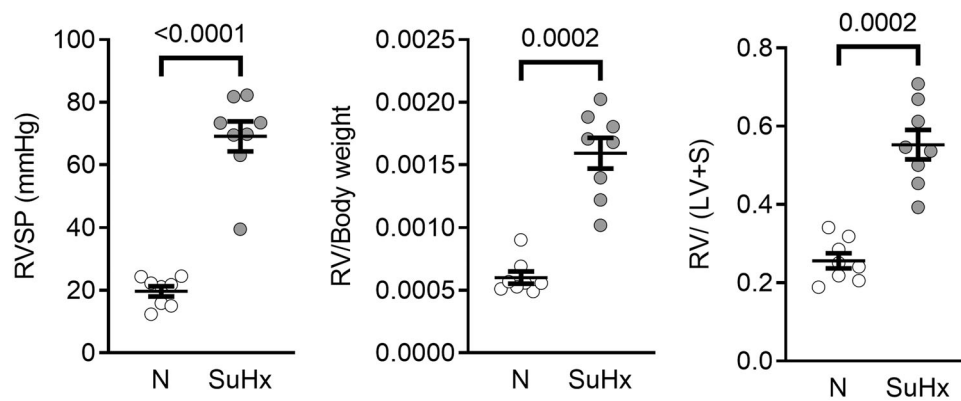


FIGURE 1 Scatter plots with mean \pm standard error of the mean (SEM) showing differences in right ventricular systolic pressure (RVSP), RV/body weight (RV/BW) and RV/LV + septum weight (RV/LV + S) in Normoxic and SuHx rats at time of serum sampling and microvascular endothelial cells harvest.

Rat RV Serum Metabolomics

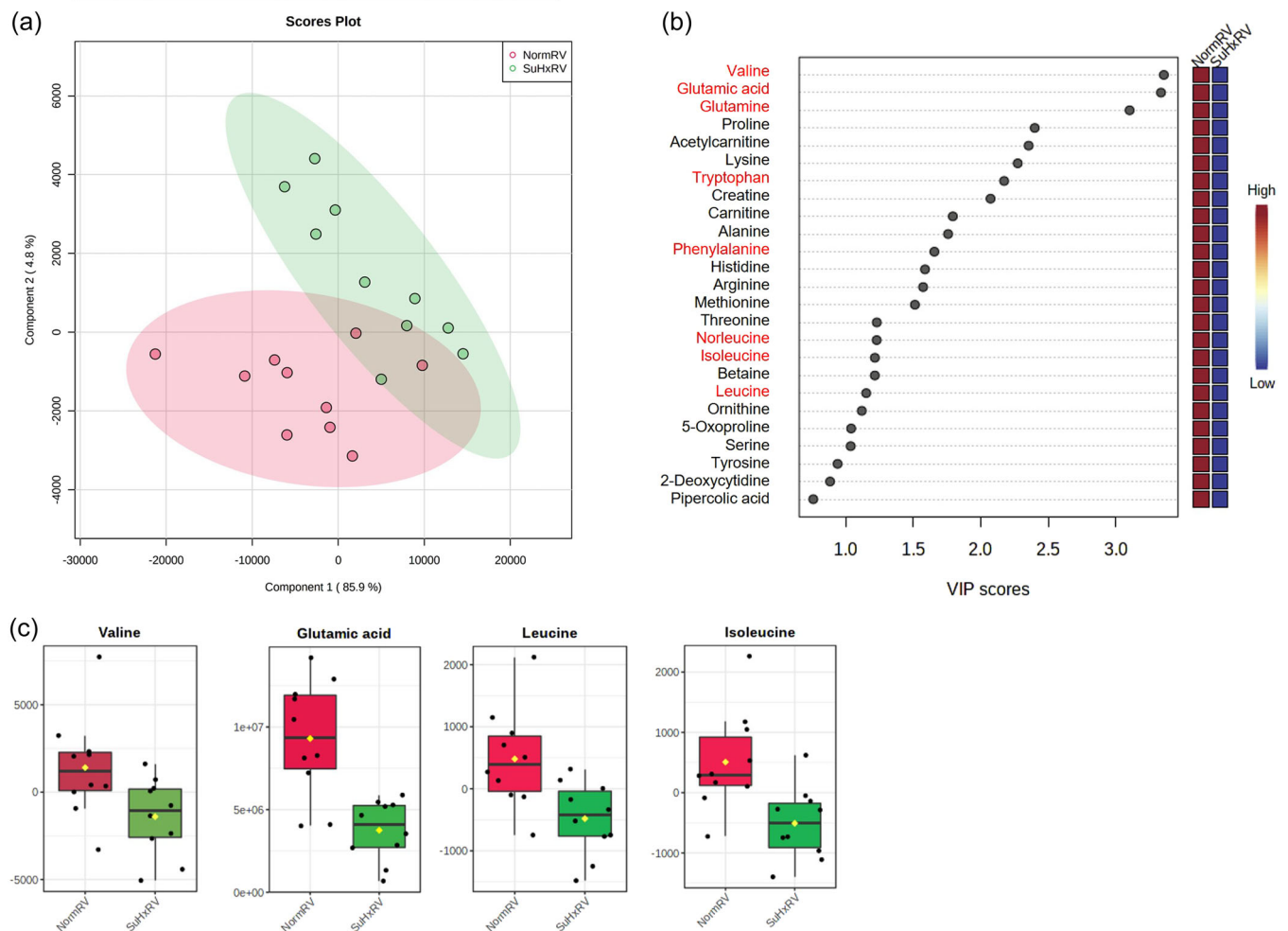


FIGURE 2 (a) Partial least squares-discriminant analysis scores plot showing differences between Normoxic and SuHx RV serum metabolite samples. Each data points represents samples from a different rat. (b) Variable importance in projection plot score both the most important variables that differentiate Normoxic and SuHx RV samples, and the direction of the difference in mean metabolite levels for each metabolite. Key metabolites are highlighted in red. (c) Box and whisker plots showing metabolite concentrations for key variables shown in the VIP plot in (b).

next examined intracellular metabolite concentrations in MVECs isolated from normoxic and SuHx rats, to understand the etiology of decreased serum RV metabolite levels. We hypothesized that intracellular levels of these metabolites would be increased, suggesting utilization of these amino acids by the pulmonary circulation.

To measure intracellular metabolites, we used cell cultures of N- and SuHx-MVECs and first performed untargeted metabolomics. The N- and SuHx- samples clustered into distinct groups (Figure 3a). When we performed PLS-DA and examined VIP scores (Figure 3b,c), we noticed that increased levels of lactic acid contributed significantly to differences between N- and SuHx-MVECs, validating our prior findings of increased intracellular lactate

concentrations and increased lactate in the supernatant of SuHx-MVECs.⁵ Next, in contrast to the serum, where glutamine levels were decreased, we observed increased levels of intracellular glutamine in our untargeted metabolomics analysis. Lastly, intracellular levels of essential amino acids like phenylalanine and the branched chain amino acid leucine were increased, as were some other nonessential amino acids such as tyrosine and arginine. This is again in contrast to the serum, where levels of many of these amino acids were decreased.

Since untargeted metabolomic analyses can be confounded by batch effects and processing, we repeated our untargeted intracellular MVEC metabolomics in a separate set of biologic replicates, and observed the same results (e.g., increased levels, in the SuHx samples, of

Rat MVEC Intracellular Metabolomics - Untargeted

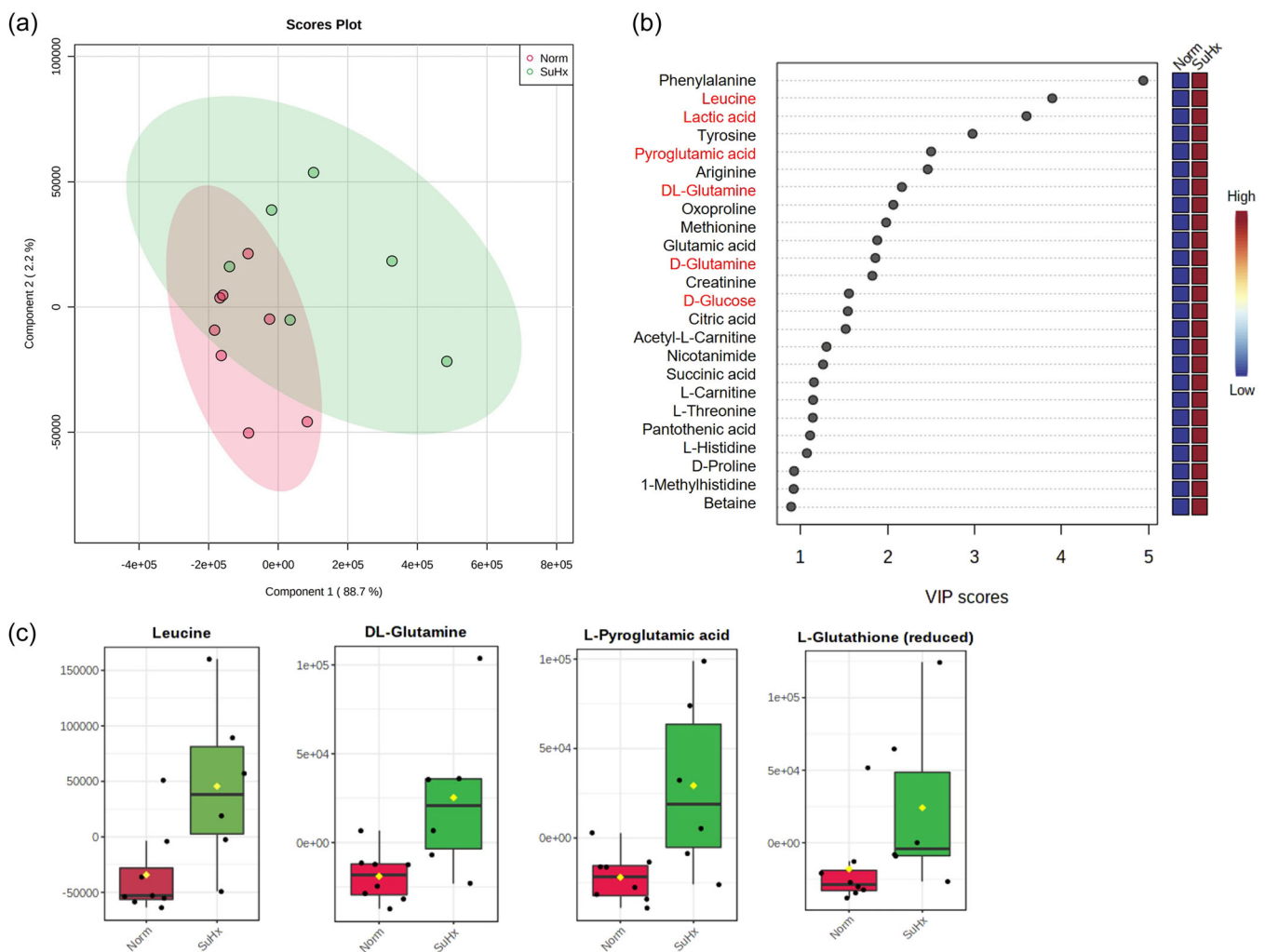


FIGURE 3 (a) Partial least squares-discriminant analysis scores plot showing differences between Normoxic and SuHx-microvascular endothelial cells (MVEC) cell lysate samples using untargeted metabolomics. (b) Variable importance in projection plot score both the most important variables that differentiate Normoxic and SuHx-MVEC lysates, and the direction of the difference in mean metabolite levels for each metabolite. Key metabolites are highlighted in red. (c) Box and whisker plots showing metabolite concentrations for key variables shown in the VIP plot in (c).

glutamine, EAAs like Phenylalanine and leucine, as well as increased intracellular lactic acid levels (Supporting Information: Figure 1). Next, we repeated these measurements using the same targeted metabolomics workflow used to measure the serum metabolites, using yet another set of different biological replicates. As shown in Figure 4, the results of targeted metabolomics measurements in intracellular lysates corroborated our untargeted metabolomics findings of increased levels of EAAs (e.g., phenylalanine and tryptophan), including several BCAAs (valine, isoleucine, leucine) in SuHx-MVECs. Taken together, these data suggest that decreased RV serum levels of amino acids in the serum of SuHx animals may be driven by increased consumption in the pulmonary vasculature. This inference is strongest for EAAs, since EAAs, by definition, cannot be produced intracellularly *de novo*. However, for other amino acids (e.g., tyrosine), it is also possible that increased intracellular levels may reflect heightened interamino acid conversion rather than increased transmembrane import.

Thus far, our RV and intracellular MVEC results still supported the notion that MVEC amino acid consumption may be occurring in the SuHx PAH model. To further understand how amino acids were being utilized by the pulmonary microvasculature, we next examined metabolite levels in the LV, comparing these findings to

the RV and MVEC lysate results. We reasoned that if amino acids were being consumed in the lung microvasculature, then levels of these amino acids would be even lower in the LV serum, and that a negative LV-RV gradient (i.e., LV/RV ratio <1) might exist in SuHx serum samples. For these analyses, the LV samples were collected concurrently with the RV samples. However, contrary to our hypothesis, LV levels of amino including glutamine were similar in normoxic and SuHx samples (Supporting Information: Figure 2). Other amino acids, such as phenylalanine, identified in our RV and intracellular analyses were not identified as significant contributors to differences between LV and RV samples in our VIP analyses. Interestingly, we did observe increased citrulline (a byproduct of nitric oxide production by endothelial nitric oxide synthase—eNOS) in SuHx LV serum samples. To determine whether transpulmonary changes in metabolite concentrations were driving differences between Normoxia and SuHx serum samples, we examined the transpulmonary metabolite gradients in our paired serum samples. We first examined the LV/RV ratio of key amino acids identified in our RV and intracellular analyses. Interestingly, as shown in Figure 5a,b, we observed positive, not negative gradients for essential amino acids like Isoleucine, leucine and phenylalanine (i.e., higher LV/RV ratios in SuHx-MVECs compared to N-MVECs). Furthermore,

Rat MVEC Intracellular Metabolomics - Targeted

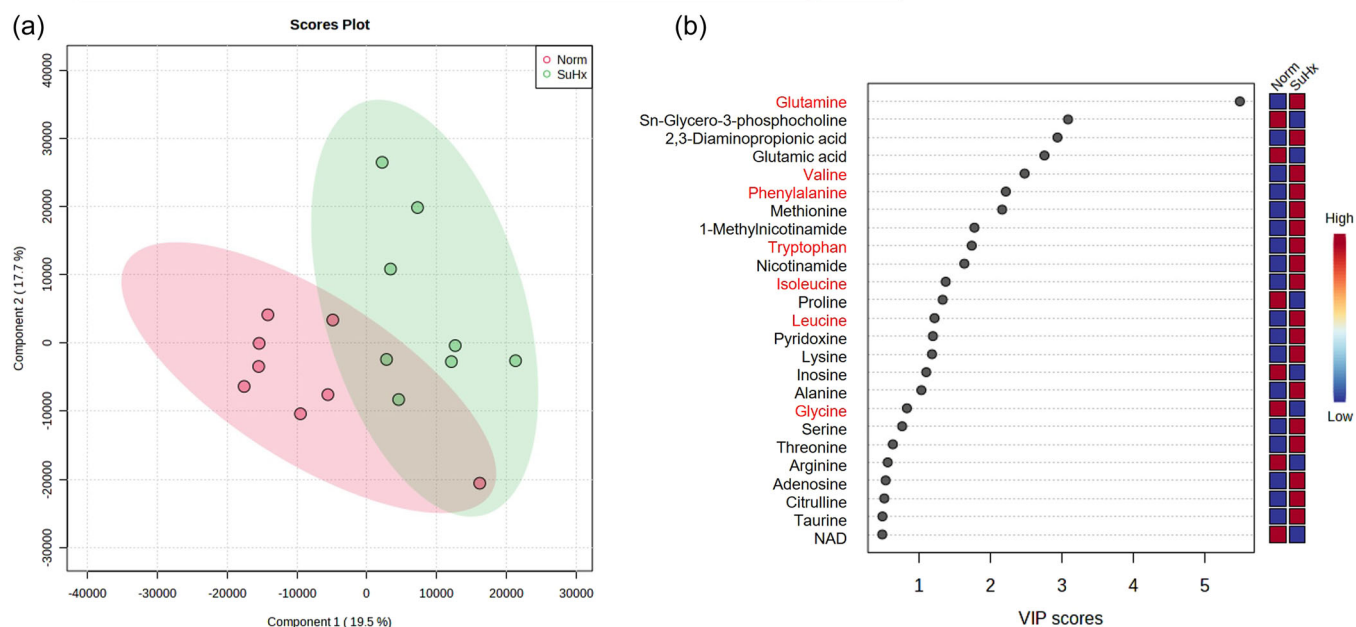


FIGURE 4 (a) Partial least squares-discriminant analysis scores plot showing differences between Normoxic and SuHx-microvascular endothelial cells (MVEC) cell lysate samples using targeted metabolomics. (b) Variable importance in projection plot score both the most important variables that differentiate Normoxic and SuHx-MVEC lysates, and the direction of the difference in mean metabolite levels for each metabolite.

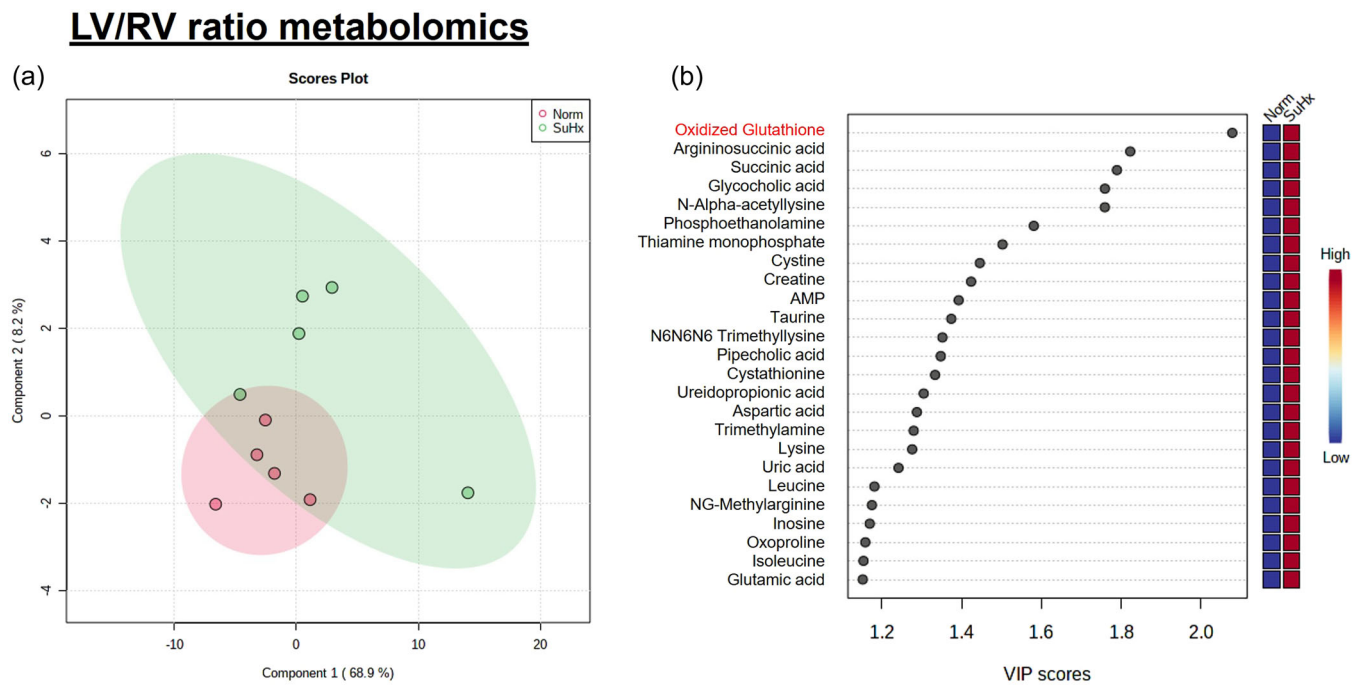


FIGURE 5 (a) Partial least squares-discriminant analysis scores plot showing differences between Normoxic and SuHx LV/RV serum metabolite ratios in samples. Each data points represents samples from a different rat. (b) Variable importance in projection plot score both the most important variables that differentiate Normoxic and SuHx LV/RV ratios.

PLS-DA of revealed that increased oxidized glutathione (i.e., increased LV/RV ratios of oxidized glutathione in SuHx) was a major determinant of the difference between the normoxic and SuHx LV/RV metabolite ratios.

Given these new findings, we hypothesized that an alternate explanation of our findings to date could be that the microvasculature could in fact be secreting, rather than consuming amino acids. This would explain why the differences present in RV serum were no longer present in LV serum. To test this hypothesis, we measured BCAA (valine, isoleucine, leucine) levels in the media supernatant of cultured N- and SuHx-MVECs. For this experiment, fresh media was added to a flask of confluent cells at time 0 and a sample of the media was collected 24 h later. As shown in Figure 6a, BCAA levels (normalized to protein levels of the cell lysates collected at the same time) in the media were higher in SuHx-MVECs compared to N-MVECs. Based on our isolation strategy and requisite phenotyping, these MVECs were microvascular in origin; however, we were unsure whether this was a global phenomenon in cells isolated from SuHx animals or whether this finding was restricted to the lung microvasculature. Since we perform a dual-step magnetic bead isolation, we compared the BCAA assay results in our lung MVECs to cultured non-MVEC (i.e., CD31⁺ cells which did not select for our MVEC marker—*Griffonia simplicifolia* isolectin). As shown in

Figure 7b, we did not observe the same pattern in these cells, arguing that the phenomenon of BCAA secretion, in the media, might be specific to lung MVECs.

Given (a) decreased RV glutamine levels (Figure 2); (b) increased MVEC intracellular glutamine and reduced glutathione levels (Figure 3); and (c) the presence of an oxidized glutathione gradient across the pulmonary vasculature (Figure 5), we hypothesized that glutamine consumption in the lung microvasculature may be driven in part by the use of glutamine to produce reduced glutathione (GSH), which becomes oxidized glutathione under conditions of increased cytoplasmic reactive oxygen species (which we have previously shown to be present in SuHx-MVECs²). Given the centrality of intracellular glutamine levels and glutamine to glutathione conversion to this hypothesis, we sought additional validation of this pathway in our metabolomics data. First, we examined whether the glutathione cycle was upregulated in SuHx-MVECs, and found that pyroglutamic acid (5-oxoproline), an intermediate in the production of glutathione from glutamine, and reduced glutathione, the end product of glutathione synthesis, was increased in SuHx lysates (Figure 3c). Second, though not contributing to the differences between groups (i.e., VIP score >1), we noted that reduced glutathione levels in the untargeted MVEC lysates was higher in the SuHx samples. Third, we directly measured the oxidized/total glutathione ratio in the media of

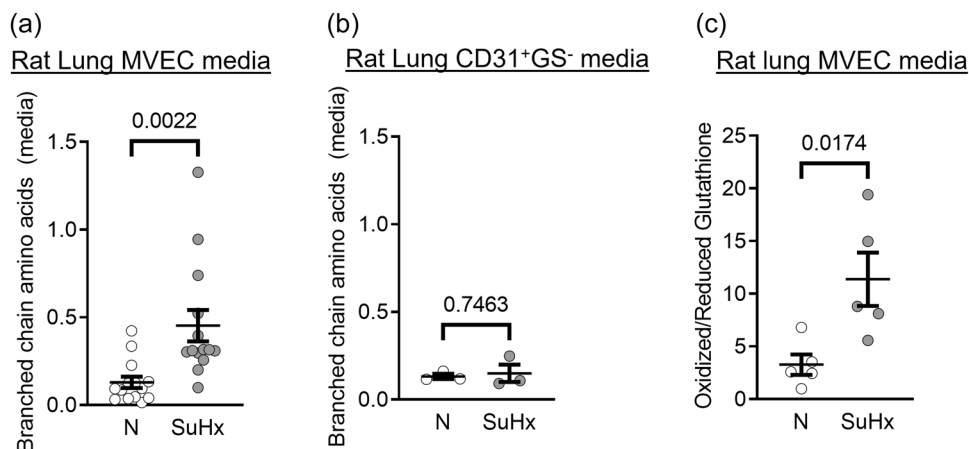


FIGURE 6 (a, b) Scatter plot (with bars showing mean \pm SEM) showing differences in branched chain amino acid concentrations in the media supernatant of cultured cells isolated from normoxic (N) or SuHx rats. Data are represented in nM BCAA/ μ g of cell lysate protein. These cells were either (a) Microvascular endothelial cells (MVECS) (Rat Lung MVECS—CD31⁺GS⁺ cells) or (b) nonmicrovascular endothelial cells (MVECS) (i.e., Rat lung CD31⁺GS⁻ cells). Each dot represents cells isolated from a different animal. (c) Scatter plot (with bars showing mean \pm SEM) showing differences in oxidized/reduced glutathione ratio (normalized to cell lysate protein concentrations) in normoxic (N) and SuHx (SuHx) rat lung MVECs. Each dot represents MVECs isolated from a different rat (i.e., biologic replicate).

Human serum metabolomics

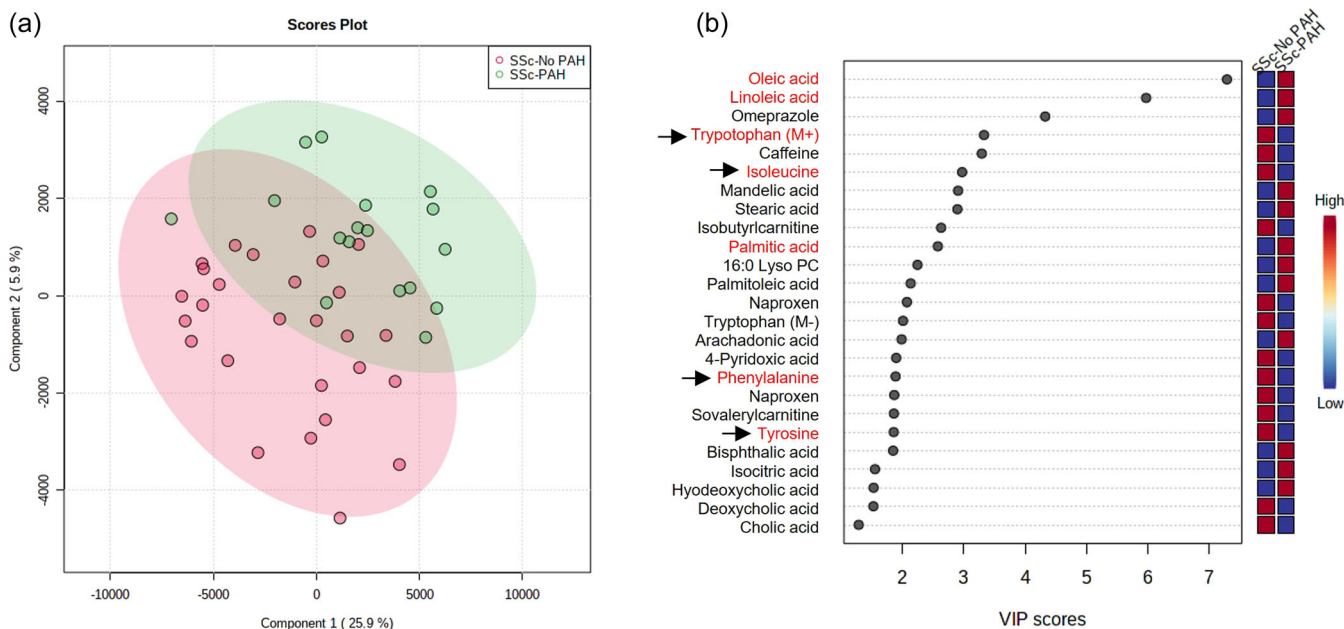


FIGURE 7 (a) Partial least squares-discriminant analysis scores plot showing differences between patients with and without systemic sclerosis (Ssc)-pulmonary artery hypertension. (b) Variable importance in projection (VIP) scores for individual metabolites. Key metabolites are highlighted in red in the VIP plot; metabolites previously measured in our animal data are highlighted with arrows.

cultured N- and SuHx-MVECs. As shown in Figure 6c, we observed increased oxidized glutathione in the SuHx-MVEC media supernatant. These additional observations corroborate that shunting of glutamine from the serum to MVECs to provide reducing equivalents of glutathione may be occurring in the pulmonary microvasculature in SuHx rats.

While the abovementioned investigation provided insight into MVEC handling of amino acids in PAH, they did not shed additional light into why concentrations of these metabolites were decreased in the RV serum. As mentioned above, this baseline difference in the pre-pulmonary circulation suggests possible systemic utilization of amino acids in SuHx. As an initial step, we sought to

first validate these intriguing rat RV serum metabolomics results in human samples. For this, we turned to metabolomic data obtained as part of a discovery metabolomics study performed in patients with Scleroderma-associated PAH (and controls), and available publicly via Metabolomics Workbench. In this study, blood samples were obtained in patients with and without systemic sclerosis (SSc)-associated PAH. Notably, this study utilized a protocol to target both non-lipid and lipid metabolites, unlike our study in SuHx rats, which focused primarily on non-lipid metabolites. The site of sample collection was the peripheral blood. Since our animal data suggests that decreased RV levels of amino acids was driven by peripheral consumption of amino acids in PAH, we hypothesized that levels of some of these amino acids (e.g., Phenylalanine, Isoleucine) would be lower in the peripheral blood of PAH patients compared to controls. Using PLS-DA, we observed that a variety of metabolites contributed to the observed differences between control and PAH serum samples (Figure 7). Of note, we repeated these analysis using using orthogonal PLS-DA and observed discrimination between groups (Supporting Information: Figure 3). We observed that the lipid compounds such as the long-chain fatty acid oleate contributed to the differences between the groups. This validated prior literature implicating abnormal serum fatty acid levels in PAH patients.¹² Importantly, we also noted that several of the amino acids (phenylalanine, isoleucine, tryptophan, tyrosine) observed to be decreased in SuHx rat serum were also decreased in PAH patient serum, and contributed to differences between control and PAH sera in this clinical cohort. (i.e., were noted to have VIP scores >1).

Our SuHx serum data and the data from our SSc patient sample cohort confirmed decreased levels of

several amino acids in the peripheral circulation of PAH patients. Reasoning that catabolism of these amino acids may be responsible for this difference, we assessed the relationship between products of BCAA catabolism and PAH severity (i.e., RVSP) using multi-variable linear regression in a second human cohort ($n = 74$ patients) of PAH patients. As shown in Table 1, some products of BCAA (and glutamine) catabolism were positively correlated with worsening PAH.

DISCUSSION

Herein, using untargeted and targeted metabolomics in animal serum, human serum, and cells isolated from rats with experimental PAH, we describe several patterns of consumption and shunting of amino acids in the pulmonary microvasculature in PAH. First, we observe decreased levels of several amino acids including BCAA (Isoleucine, leucine, valine), phenylalanine and glutamine in the RV serum of SuHx rats and in serum samples from PAH patients. If taken with our MVEC intracellular metabolomics data demonstrating increased intracellular levels of these metabolites, these findings suggest increased consumption of amino acids in the lung microvasculature. However, when these data are paired with our LV, transpulmonary gradient, and media supernatant metabolite measurements, a different picture emerges. In sum, our data suggest that secretion of amino acids into the blood stream may also be occurring at additional points in the lung microvasculature. We had initially reasoned that the decreased RV serum amino acids were due to increased MVEC consumption; however, in light of the LV data, we now posit that amino acid consumption by peripheral tissues (e.g., muscle), or

TABLE 1 Association between products of amino acid catabolism and RVSP.

Model	Metabolite	Pathway	p Value	Direction of relationship
Unadjusted	2-methylmalonylcarnitine (C4-DC)	BCAA Metabolism	0.026	Positive
Adjusted with age, sex, BMI, and PAH etiology (our metric of disease severity)	alpha-ketoglutarate	Glutamate Metabolism	0.0052	Positive
	2-methylmalonylcarnitine (C4-DC)	BCAA Metabolism	0.0074	Positive
	N-carbamoylvaline	Leucine, isoleucine and valine metabolism	0.020	Positive
	4-hydroxyphenylacetylglutamine	Acetylated peptides	0.035	Positive
	N-acetyl-aspartyl-glutamate (NAAG)	Glutamate metabolism	0.040	Positive
	Phenylacetylglutamine	Acetylated peptides	0.041	Positive

Note: Results of univariate and multi-variable linear regression assessing the relationship between peripheral blood levels of products of BCAA and glutamine catabolism and PAH severity (RVSP) in a cohort of PAH patients ($n = 74$).

Abbreviations: BCAA, branched chain amino acid; BMI, body mass index; PAH, pulmonary artery hypertension.

the RV itself, may in fact be responsible for the amino acid differences observed in the pre-capillary circulation.

In addition to shedding light on the consumption/secretion of essential amino acids, our data also provide evidence of how glutamine may be utilized in MVECs in PAH. Though intracellular glutamine levels are high in SuHx-MVECs, our gradient data suggests that glutamine is being used for glutathione synthesis. In other words, the presence of a positive (i.e., increased LV/RV ratio) oxidized glutathione gradient across the pulmonary vasculature, paired with increased intracellular glutamine and reduced glutathione levels argues that increased microvascular glutamine consumption is being used to produce glutathione. This is interesting because while a central role of EC glutamine in PAH has been previously described, it has largely been assumed that this was due to the use of glutamine as an anaplerotic fuel source to generate alpha-ketoglutarate. While our data does that discount that possibility, it additionally suggests that glutamine may be playing a role in regulating MVEC redox balance, and that increased glutamine consumption may occurring in part to produce reducing equivalents of glutathione, and offset chronic MVEC oxidant stress.

On first glance, our findings of possible glutamine shunting (to glutathione) and increased intracellular essential amino acids seem logically related. Depriving cells of glutamine for anaplerotic carbons may favor utilization of other amino acids (phenylalanine, tyrosine, isoleucine) that we observed to be (1) decreased in the RV serum and (2) increased intracellularly in SuHx-MVECs lysates. In isolation, these portions of our data suggest that while MVEC glutamine is being used to provide glutathione and maintain redox homeostasis, other amino acids may be providing anaplerotic carbons to sustain the TCA cycle in its absence. However, as detailed below, the exact nature of amino acid flux in the lung MVECs appears to be more complicated than simply one of MVEC consumption.

Based on our RV and intracellular data, we would expect that SuHx LV serum concentrations of valine and other EAAs would be even lower than the RV concentrations. However, we observe the opposite. While the reason for this discrepancy is still not fully clear, our transpulmonary gradient data, taken with our data suggesting increased, rather than decreased, BCAA levels in the SuHx-MVEC cell culture media at 24 h, suggests that SuHx-MVECs may in fact be secreting these amino acids.

We attempted to localize the source of amino acid secretion by exploiting the cells generated by our dual-step MVEC isolation process. By comparing the media supernatant of CD31⁺GS⁺ (i.e., microvascular) cells to

CD31⁺GS⁻ cells, we hoped to better understand whether our observed differences in BCAA levels were specific to MVECs or a more global phenomenon. On the one hand, the presence of a difference in the MVEC media (but not CD31⁺GS⁻ cell culture media) suggests that, if in fact BCAA secretion is occur *in vivo*, it may not be occurring across the entire lung endothelium. One caveat to these data is that CD31⁺GS⁻ cells likely represent a heterogeneous population of cells; while some of these cells are likely macrovascular ECs, other CD31⁺ nonendothelial cells (including immune cells) may also be included in this population. Therefore, while these data are provocative, the question of the exact source and mechanism of amino acid release within the lung microvasculature still requires further investigation.

Our analysis of human serum data show that while amino acids levels are lower in the venous blood, fatty acid levels are higher. One possibility is that increased utilization of fatty acids for anaplerotic carbons may free up amino acids for participation in protein synthesis and, as our MVEC culture data suggest, secretion from MVECs. Our finding of increased fatty acids in the sera of human PAH patients is consistent with prior reports^{12,13} Our observation that similar amino acids are lower in both the RV of rats and the peripheral blood of humans suggests that our RV serum findings are not unique to the SuHx rat and may phenocopy human serum findings. Furthermore, our findings of an positive, significant association between products of BCAA catabolism and PAH severity in a second cohort of patients suggests that peripheral catabolism (with subsequent replenishment via the pulmonary vasculature) of BCAA may be occurring in PAH.

In contrast to our study, Lin et al found an increase, rather than decrease in serum levels of EAA (including leucine and isoleucine) in rat serum following exposure to the monocrotaline (MCT) PH model,¹⁴ a difference that could be reflection of either differences in PH severity induced by the two models and/or technical differences in measurement methodology (H-NMR vs. MS). On the other hand, two studies in humans note results similar to ours with regard to the relationship between serum BCAA levels and PAH. In a study involving 52 PAH patients undergoing serum metabolomics, Mey et al noted decreased levels of several amino acids including isoleucine and leucine.¹⁵ Similarly, Rhodes et al showed that lower plasma valine levels were associated with worse mortality in both a discovery and validation cohort of PAH patients.¹⁶ These studies, taken with our data, suggest a role for peripheral BCAA catabolism and possible lung microvasculature secretion of BCAA in PAH pathobiology. However, whether this

process is causal in promoting EC pathobiology in PAH requires further investigation.

There are several limitations to this study. While these data highlight the importance of amino acid metabolism to the SuHx model of PAH, further metabolomic studies (such as ¹³C labeling experiments) are needed to determine the exact destination of serum amino acids in PAH models. Next, while our RV and LV serum samples reflect the *in vivo* situation, our intracellular metabolomics data is confounded by time spent in culture. This was done largely for technical reasons; direct isolation of ECs from the intact lung (i.e., magnetic bead isolation followed by direct suspension in metabolomic extraction media, rather than cell culture) did not yield, in our hands, enough MVECs in high enough concentrations for metabolomic extractions. Therefore, the possibility exists that the intracellular data may be confounded by the changes in metabolite concentrations in the cell culture media (in comparison to serum). Lastly, while our data suggests a variety of metabolic shifts in MVECs, the cellular functional consequences of the various changes require exploration; whether shunts such as glutamine and glutathione and export of BCAA are simply epiphenomena of proliferative MVECs in PAH or whether they are causal in promoting sustained proliferation of these cells *in vitro* (as described by us⁷ and others¹⁷ previously) remains unknown. Longitudinal examination of the the serum (and MVEC) metabolome using earlier time points in the the SuHx model will be useful to better understand how BCAA levels may be impacting EC dysfunction in PAH.

In conclusion, our data provide new insight into amino acid metabolite regulation across the pulmonary vasculature in a relevant model of PAH. These data provide the foundation for more mechanistic studies aimed at understanding how interrupting glutathione and/or branched-chain amino acid metabolism in MVECs alters cellular and/or organ dysfunction in PAH.

AUTHOR CONTRIBUTIONS

Data collection: Nicolas Philip, Hongyang Pi, Mahin Gadkari, Xin Yun, John Huetsch, Cissy Zhang, Aurelie Roux, David Graham, Karthik Suresh, Peter J. Leary, and Sina A. Gharib. **Conceptualization and experimental design:** Hongyang Pi, John Huetsch, Robert Harlan, David Graham, Larissa Shimoda, Anne Le, Scott Visovatti, Catherine Simpson, Lakshmi Santhanam, Jochen Steppan, Peter J. Leary, Sina A. Gharib, and Karthik Suresh. **Data analysis:** Hongyang Pi, Mahin Gadkari, Robert Harlan, Aurelie Roux, David Graham, Anne Le, and Scott Visovatti. **Figure preparation:** Karthik Suresh, Hongyang Pi, and Nicolas Philip. **Writing manuscript:** Karthik Suresh, Jochen Steppan, Larissa Shimoda,

Catherine Simpson, Anne Le, Scott Visovatti, Lakshmi Santhanam, David Graham, and Robert Harlan. **Interpretation of data:** All authors. **Editing and providing input on manuscript:** All authors.

ACKNOWLEDGMENTS

Funding sources: R01HL151530 (Karthik Suresh), K08132055 (Karthik Suresh), R01HL126514 (Lakshmi Santhanam), K08HL145132 (Lakshmi Santhanam), K23HL153781 (Catherine Simpson), K08HL133475 (John Huetsch).

CONFLICT OF INTEREST STATEMENT

The authors declare no conflict of interest.

ETHICS STATEMENT

All procedures were approved by the Johns Hopkins University School of Medicine Animal Care and Use Committee. All studies involving humans were approved the local institutional review board.

ORCID

Mahin Gadkari  <https://orcid.org/0000-0002-9214-8656>

Catherine Simpson  <http://orcid.org/0000-0002-2388-5660>

Karthik Suresh  <https://orcid.org/0000-0003-2920-0949>

REFERENCES

- Mammoto T, Muyleart M, Konduri GG, Mammoto A. Twist1 in hypoxia-induced pulmonary hypertension through transforming growth factor- β -smad signaling. *Am J Respir Cell Mol Biol.* 2018;58(2):194–207. <https://doi.org/10.1165/rcmb.2016-0323oc>
- Suresh K, Servinsky L, Jiang H, Bigham Z, Yun X, Kliment C, Huetsch J, Damarla M, Shimoda LA. Reactive oxygen species induced Ca²⁺ influx via TRPV4 and microvascular endothelial dysfunction in the SU5416/hypoxia model of pulmonary arterial hypertension. *Am J Physiol Lung Cell Mol Physiol.* 2018;314(5):L893–907. <https://doi.org/10.1152/ajplung.00430.2017>
- Ryan J, Dasgupta A, Huston J, Chen KH, Archer SL. Mitochondrial dynamics in pulmonary arterial hypertension. *J Mol Med.* 2015;93:229–42. <https://doi.org/10.1007/s00109-015-1263-5>
- Xu W, Janocha AJ, Erzurum SC. Metabolism in pulmonary hypertension. *Annu Rev Physiol.* 2021;83(1):551–76. <https://doi.org/10.1146/annurev-physiol-031620-123956>
- Suresh K, Servinsky L, Jiang H, Bigham Z, Zaldumbide J, Huetsch JC, Kliment C, Acoba MG, Kirsch BJ, Claypool SM, Le A, Damarla M, Shimoda LA. Regulation of mitochondrial fragmentation in microvascular endothelial cells isolated from the SU5416/hypoxia model of pulmonary arterial hypertension. *Am J Physiol Lung Cell Mol Physiol.* 2019;317:L639–52. <https://doi.org/10.1152/ajplung.00396.2018>
- Chouvarine P, Giera M, Kastenmüller G, Artati A, Adamski J, Bertram H, Hansmann G. Trans-right ventricle and transpulmonary metabolite gradients in human pulmonary arterial

- hypertension. *Heart*. 2020;106:1332–41. <https://doi.org/10.1136/heartjnl-2019-315900>
7. Suresh K, Servinsky L, Jiang H, Bigam Z, Yun X, Kliment C, Huetsch J, Damarla M, Shimoda LA. Reactive oxygen species induced Ca^{2+} influx via TRPV4 and microvascular endothelial dysfunction in the SU5416/hypoxia model of pulmonary arterial hypertension. *Am J Physiol Lung Cell Mol Physiol*. 2018;314:L893–907. <https://doi.org/10.1152/ajplung.00430.2017>
 8. Huetsch JC, Jiang H, Larrain C, Larrain C, Shimoda LA, The Na^+/H^+ exchanger contributes to increased smooth muscle proliferation and migration in a rat model of pulmonary arterial hypertension. *Physiol Rep*. 2016;4:e12729. <https://doi.org/10.14814/phy2.12729>
 9. Suresh K, Servinsky L, Reyes J, Udem C, Zaldumbide J, Rentsendorj O, Modekurty S, Dodd-o JM, Scott A, Pearse DB, Shimoda LA. CD36 mediates H_2O_2 -induced calcium influx in lung microvascular endothelial cells. *Am J Physiol Lung Cell Mol Physiol*. 2017;312:L143–53. <https://doi.org/10.1152/ajplung.00361.2016>
 10. Suresh K, Servinsky L, Reyes J, Baksh S, Udem C, Caterina M, Pearse DB, Shimoda LA. Hydrogen peroxide-induced calcium influx in lung microvascular endothelial cells involves TRPV4. *Am J Physiol Lung Cell Mol Physiol*. 2015;309:L1467–77. <https://doi.org/10.1152/ajplung.00275.2015>
 11. Alvarez DF, Huang L, King JA, ElZarrad MK, Yoder MC, Stevens T. Lung microvascular endothelium is enriched with progenitor cells that exhibit vasculogenic capacity. *Am J Physiol Lung Cell Mol Physiol*. 2008;294:L419–30. <https://doi.org/10.1152/ajplung.00314.2007>
 12. Hemnes AR, Luther JM, Rhodes CJ, Burgess JP, Carlson J, Fan R, Fessel JP, Fortune N, Gerszten RE, Halliday SJ, Hekmat R, Howard L, Newman JH, Niswender KD, Pugh ME, Robbins IM, Sheng Q, Shiba CA, Shyr Y, Sumner S, Talati M, Wharton J, Wilkins MR, Ye F, Yu C, West J, Brittain EL. Human PAH is characterized by a pattern of lipid-related insulin resistance. *JCI Insight*. 2019;4(1):e123611. <https://doi.org/10.1172/jci.insight.123611>
 13. Chen C, Luo F, Wu P, Huang Y, Das A, Chen S, Chen J, Hu X, Li F, Fang Z, Zhou S. Metabolomics reveals metabolite changes of patients with pulmonary arterial hypertension in China. *J Cell Mol Med*. 2020;24(4):2484–96. <https://doi.org/10.1111/jcmm.14937>
 14. Lin T, Gu J, Huang C, Zheng S, Lin X, Xie L, Lin D. 1H NMR-based analysis of serum metabolites in monocrotaline-induced pulmonary arterial hypertensive rats. *Dis Markers*. 2016;2016:1–11. <https://doi.org/10.1155/2016/5803031>
 15. Mey JT, Hari A, Axelrod CL, Fealy CE, Erickson ML, Kirwan JP, Dweik RA, Heresi GA. Lipids and ketones dominate metabolism at the expense of glucose control in pulmonary arterial hypertension: a hyperglycaemic clamp and metabolomics study. *Eur Respir J*. 2020;55(4):1901700. <https://doi.org/10.1183/13993003.01700-2019>
 16. Rhodes CJ, Ghataorhe P, Wharton J, Rue-Albrecht KC, Hadinnapola C, Watson G, Bleda M, Haimel M, Coghlan G, Corris PA, Howard LS, Kiely DG, Peacock AJ, Pepke-Zaba J, Toshner MR, Wort SJ, Gibbs JSR, Lawrie A, Gräf S, Morrell NW, Wilkins MR. Plasma metabolomics implicates modified transfer RNAs and altered bioenergetics in the outcomes of pulmonary arterial hypertension. *Circulation*. 2017;135(5):460–75. <https://doi.org/10.1161/circulationaha.116.024602>
 17. Humbert M, Montani D, Perros F, Dorfmueller P, Adnot S, Eddahibi S. Endothelial cell dysfunction and cross talk between endothelium and smooth muscle cells in pulmonary arterial hypertension. *Vascul Pharmacol*. 2008;49:113–8. <https://doi.org/10.1016/j.vph.2008.06.003>

SUPPORTING INFORMATION

Additional supporting information can be found online in the Supporting Information section at the end of this article.

How to cite this article: Philip N, Pi H, Gadkari M, Yun X, Huetsch J, Zhang C, Harlan R, Roux A, Graham D, Shimoda L, Le A, Visovatti S, Leary PJ, Gharib SA, Simpson C, Santhanam L, Steppan J, Suresh K. Transpulmonary amino acid metabolism in the sugen hypoxia model of pulmonary hypertension. *Pulm Circ*. 2023;13:e12205. <https://doi.org/10.1002/pul2.12205>